Clay Minerals, (2018) **53**, 497–503

Flow supercritical synthesis of brucite and magnesian T-O, T-O-T phyllosilicates: an opportunity to tune the structure with the solvent composition

MARIE CLAVERIE[1], FRANÇOIS MARTIN[2,*], CHRISTEL CAREME[1], CHRISTOPHE LE ROUX[2], PIERRE MICOUD[2], OLIVIER GRAUBY[3] AND CYRIL AYMONIER[4]

[1] *Imerys, 2 Place Édouard Bouillères, Toulouse, 31100, France*
[2] *Géosciences Environnement Toulouse (GET, UMR 5563, UPS-CNRS-IRD-CNES, ERT 1074 Géomatériaux), 14 Avenue Édouard Belin, Toulouse, 31400, France*
[3] *Aix Marseille Université, CNRS, CINaM UMR 7325, Campus de Luminy, Marseille, 13288, France*
[4] *CNRS, Univ. Bordeaux, ICMCB, UPR 9048, Pessac, 33600, France*

(*Received 30 October 2017; revised 25 June 2018; Editor: G. E. Christidis*)

ABSTRACT: This work presents the synthesis of minerals with a layered structure in supercritical water/ethanol mixtures to decrease the critical coordinates of the solvent regarding water. Depending on the water/ethanol ratio of the solvent, we obtained three different minerals adopting an octahedral brucitic sheet: (1) without a Si-tetrahedral sheet (O); (2) associated with one Si-tetrahedral sheet (T-O); or (3) intercalated between two Si-tetrahedral sheets (T-O-T). We have thus shown that ethanol in a supercritical water/ethanol mixture changes the solubility of silicon with a direct consequence on the formation of the tetrahedral silicon sheets and thus makes it possible to control the structure of the synthesized layered material.

KEYWORDS: phyllosilicates, brucite, continuous-flow synthesis, supercritical water/ethanol mixtures.

Layered minerals are omnipresent in nature and are used in a wide variety of applications; for example, as mineral fillers in composite materials such as polymers, paints, *etc*. (Konta, 1995; Zazenski *et al.*, 1995; Murray, 2000; Ding *et al.*, 2001; Carretero, 2002). Despite their applications, they have some disadvantages (heterogeneous particle sizes and chemical compositions, presence of impurities) that may restrict their use, especially for fine chemicals or petrochemicals (Bergaya & Lagaly, 2006). To overcome these drawbacks, the synthesis of phyllosilicates such as talc ($Si_4Mg_3O_{10}(OH)_2$) was envisaged by scientists in the last century (Claverie *et al.*, 2018).

The synthesis of phyllosilicates plays an important role in the development of new materials. Since 2015, there has been a renewed interest in extending mineral synthesis for industrial purposes (Schaef *et al.*, 2015; Dumas *et al.*, 2016; Diez-Garcia *et al.*, 2017; Cecilia *et al.*, 2018; Cirillo *et al.*, 2018). In those studies, the innovative process highlighted combines a continuous set-up with the use of supercritical water for the synthesis of talc ($Si_4Mg_3O_{10}[OH]_2$) and tobermorite

This paper was originally presented during the session: 'NT-10 Recent advances in applications of industrial clays' of the International Clay Conference 2017.
*E-mail: francois.martin@get.omp.eu; cyril.aymonier@icmcb.cnrs.fr
https://doi.org/10.1180/clm.2018.36

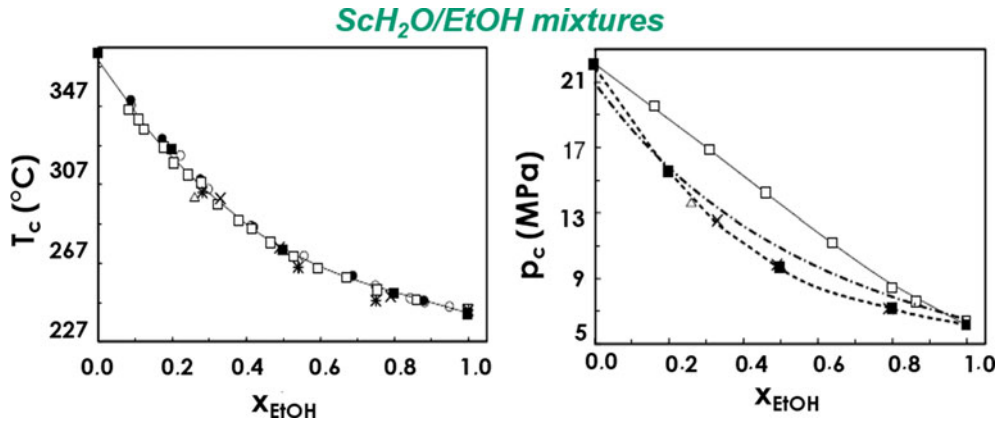

FIG. 1. Evolution of the critical T and p as a function of the water/ethanol mixture composition. ●: data from Marshall & Jones (1974); □: data from Griswold *et al*. (1943); ×: data from Barr-David & Dodge (1959); ■: data from Bazaev *et al*. (2007). Reprinted with permission from Elsevier (from Bazaev *et al.*, 2007).

($Ca_5Si_6O_{16}(OH)_2.nH_2O$). In a general way, the supercritical solvothermal synthesis underlines the advantage of combining a fast process (a few seconds compared with hours to many days for a batch synthesis) with an opportunity to scale up the process.

This study adopts a new strategy in phyllosilicate supercritical synthesis with the use of a different solvent: a water/ethanol mixture. Interactions between water and ethanol allowed modification of the critical temperature and pressure of the solvent as shown in Fig. 1 (critical coordinates of ethanol: $T_c = 241°C$, $p_c = 6.27$ MPa; critical coordinates of water: $T_c = 374°C$, $p_c = 22.06$ MPa). This phenomenon is due to the change in water molecule organization when ethanol is added (Griswold *et al.*, 1943; Laaksonen *et al.*, 1997; Bazaev *et al.*, 2007).

This study reports the influence of the composition of the water/ethanol mixture on the structure of the phyllosilicates formed. Various types of phyllosilicates were synthesized using a continuous-flow reactor described in a recent patent (Aymonier *et al.*, 2015) and developed at the Institut de Chimie de la Matière Condensée de Bordeaux (ICMCB) laboratory for the synthesis of different types of materials, such as oxides, metals, nitrides, *etc*. (Fig. 2) (Aymonier *et al.*, 2018).

To perform the phyllosilicate synthesis, two separate injection lines of solutions were used. One involved

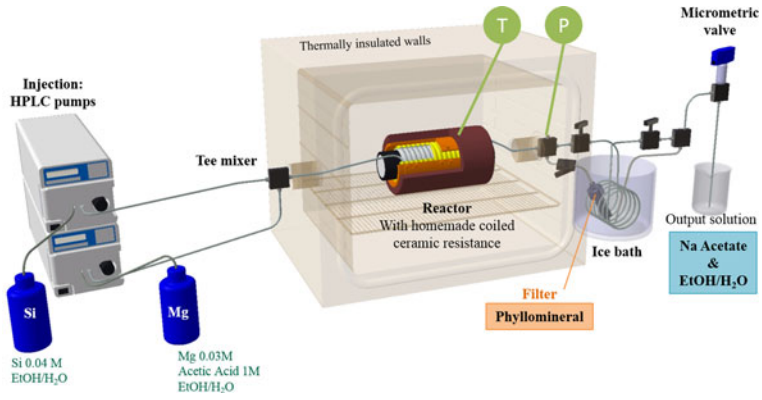

FIG. 2. Custom-built continuous process used for synthesis of layered minerals under supercritical conditions. T = thermocouple; P = manometer; HPLC = high-performance liquid chromatography. Reprinted with permission from Wiley-VCH (from Dumas *et al.*, 2016).

https://doi.org/10.1180/clm.2018.36 Published online by Cambridge University Press

TABLE 1. Synthesis conditions of layered mineral samples. The nomenclature of samples in the present study is in the form X-N%, where X represents the first letter of the mineral obtained (M for mica, S for serpentine and B for brucite) and N is the ethanol content.

Sample name	Reaction medium = ethanol/water (mol.% EtOH in reaction medium)	Temperature (°C)	Pressure (MPa)	Synthesis duration (s)	Conditions
M-0%	0	400	25	20	Supercritical conditions
M-5%	5	”	”	”	”
M-10%	10	”	”	”	”
M-20%	20	”	”	”	”
S-28%	28	”	”	”	”
B-50%	50	”	”	”	”

0.03 M magnesium acetate ($Mg(CH_3COO)_2.4H_2O$) and 1 M acetic acid in the water/ethanol mixture and the second involved 0.04 M potassium silicate ($K_2SiO_3.nH_2O$) in the water/ethanol mixture. These two solutions were mixed separately at room temperature before being injected into the reactor *via* a tee mixer point. The reactor, made of 1/8 inch, 316 L stainless steel coiled tubing, has an internal diameter of 1.57 mm for a total volume of 8 cm^3. The temperature (up to 500°C) was controlled by a homemade coiled ceramic resistor. The pressure is consistent throughout the whole system, monitored using manometers and controlled with a micrometre needle valve (Autoclave Engineers). In the reactor operating at supercritical conditions, the formation of phyllosilicate particles occurs. An ice bath, placed downstream of the reactor, allows thermal quenching of the reaction. The phyllosilicate product was recovered in a filter, while the solvent solution containing salt was collected for reuse after depressurization through the micrometric valve. The pressure was set to 25 MPa, the temperature to 400°C and the residence time was fixed at 20 s in each experiment. The appropriate flow rate Q ($m^3\ s^{-1}$) for a residence time of 20 s at 400°C and 25 MPa has

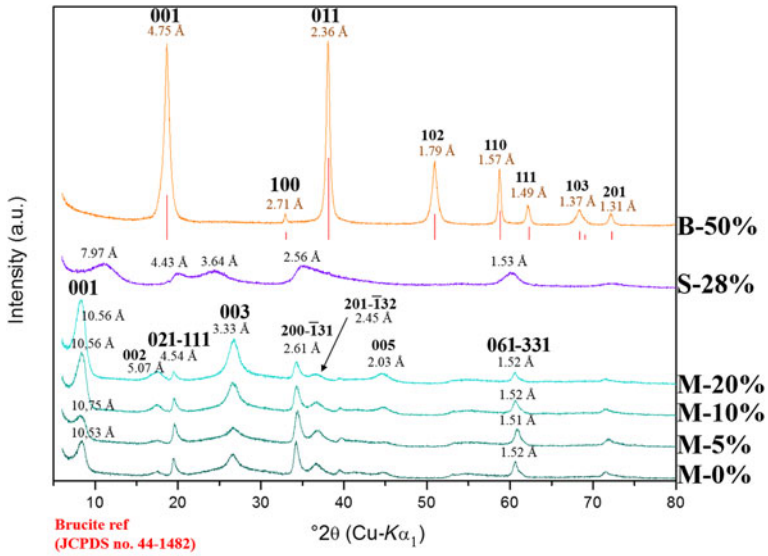

FIG. 3. Powder XRD patterns of minerals synthesized at 400°C and 25 MPa in 20 s with various amounts of ethanol.

https://doi.org/10.1180/clm.2018.36 Published online by Cambridge University Press

been calculated for each solvent mixture using the following equation:

$$Q = \frac{V_{\text{reactor}} \times \rho_r}{\tau \times \rho_i} \quad (1)$$

where τ is the residence time, V_{reactor} is the volume of the reactor and ρ_i and ρ_r are the solvent mixture densities at a pressure of 25 MPa and temperatures of 25°C and 400°C, respectively.

One set of samples was obtained to investigate the role of the water/ethanol molar ratio under supercritical conditions at 400°C (nomenclature and description of the samples are given in Table 1). Figure 3 illustrates the X-ray diffraction (XRD) patterns of powdered samples synthesized at 25 MPa for ~20 s by varying the ethanol content in the reaction medium from 0 to 50 mol.%. The ethanol content of the reaction medium drastically affects the nature of the phase synthesized. Indeed, at a lower ethanol content (<20 mol.%), the tetrasilicic magnesium mica ($KSi_4(Mg_{2.5}\square_{0.5})O_{10}(OH)_2$; TMM) structure was developed. Mica was synthesized using potassium silicate as the silicon source. The crystal order of these samples increased with the ethanol content (from 0 to 20 mol.%).

By contrast, when synthesis was performed in a reaction medium composed of 28 mol.% ethanol, the XRD patterns of the end product indicated a poorly crystallized phyllosilicate structure (reflections at

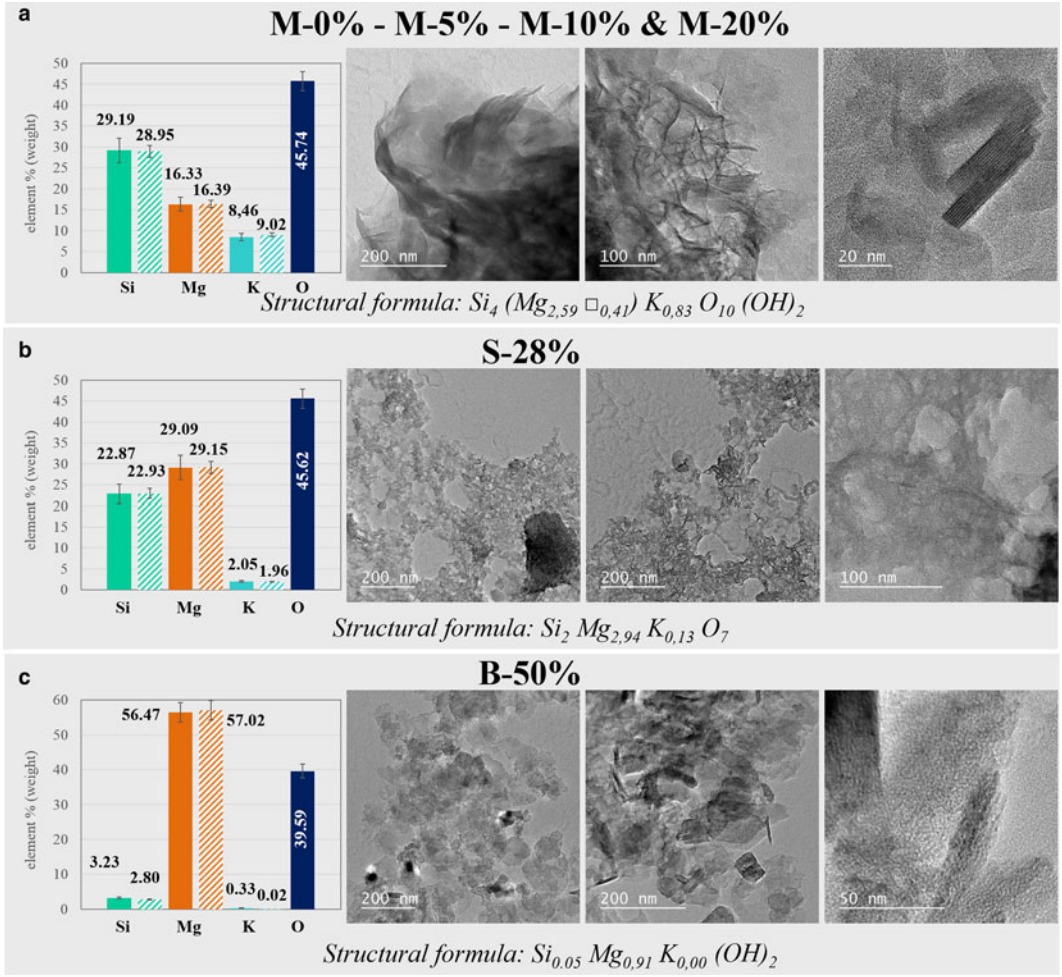

FIG. 4. Chemical analyses by electron microprobe (solid bars) and by ICP-AES (hatched bars) and transmission electron microscopy images of (a) M-0%, M-5%, M-10% and M-20%, (b) S-28% and (c) B-50%.

https://doi.org/10.1180/clm.2018.36 Published online by Cambridge University Press

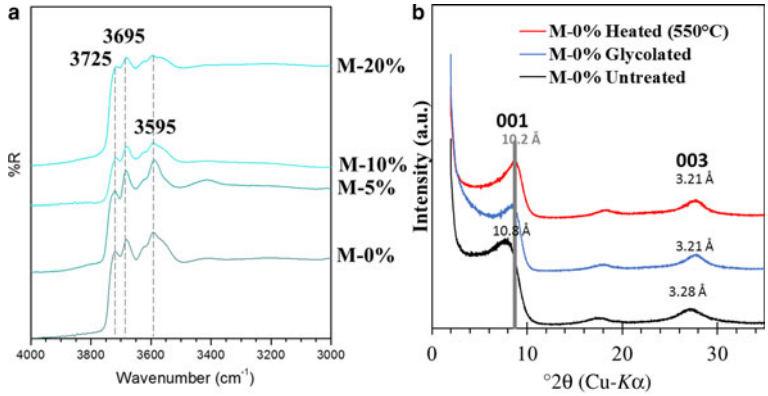

FIG. 5. (a) MIR spectra of mica solid samples in the OH-stretching region. (b) X-ray diffraction patterns of the oriented aggregate sample M-0% untreated, glycolated and heated at 550°C.

~7.97 and 1.53 Å) (Grauby *et al.*, 1998) and the absence of mica. Moreover, 001 reflections shifted towards large angles, indicating a decrease in the interlayer distance (Fig. 3). The S-28% sample is designated as a 1:1 serpentine-like phyllosilicate with an elementary layer of ~8 Å. Lastly, sample B-50%, synthesized in a reaction medium composed of 50 mol.% of ethanol, exhibits all reflection characteristics of a brucite structure (JCPDS no. 44-1482, space group $\overline{P3}m1$ with unit-cell parameters of $a = 3.144$ Å and $c = 4.777$ Å). These first XRD results reveal an evolution of the tetrahedral–octahedral–tetrahedral arrangements with the ethanol content in the reaction medium.

Complementary analyses with transmission electron microscopy (TEM) and electron microprobe analysis confirmed by inductively coupled plasma-atomic emission spectroscopy (ICP-AES) allowed precise identification of the nature of the three main minerals obtained (Fig. 4). For synthesis in a reaction medium containing <20 mol.% ethanol, TEM images present a sample with folded and tortuous very thin sheets up to 200 nm in diameter. The microprobe analysis shows a Si/Mg weight ratio of ~1.78 (equivalent to an atomic ratio Si/Mg of ~1.54) and 8.46 wt.% potassium. The atomic Si/Mg ratio of 1.54 is in agreement with the presence of mica (Figs 3, 4). This ratio differs from the 4:3 injected into the tee mixer, confirming the influence of the solvent composition on the material formed. The Mg deficit created octahedral vacancies and induced a negative charge to the layers. Subsequently, K from the silicon source was

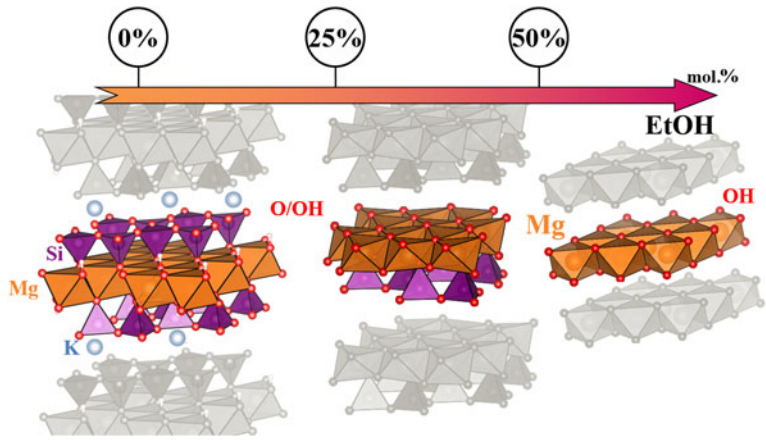

FIG. 6. Schematic diagram of mineral synthesis in a supercritical water/ethanol mixture.

https://doi.org/10.1180/clm.2018.36 Published online by Cambridge University Press

introduced in the interlayer space. Mid-infrared (MIR) spectra in the hydroxyl stretching zone of these samples are presented in Fig. 5a. The spectra of the M-N% samples in the OH-stretching region consist of two N-bands at 3725 and 3695 cm^{-1} corresponding to the OH bonded to $3Mg^{2+}$ and one V-type band at 3595 cm^{-1} corresponding to the OH adjacent to an octahedral vacancy of a TMM (Robert & Kodama, 1988; Robert *et al.*, 1993). Moreover, to confirm the non-swelling nature of the particles synthesized in a reaction medium containing <20 mol.% of ethanol, various treatments were performed on the oriented aggregate samples: untreated, ethylene glycol solvated and heated at 550°C (Fig. 5b). The respective 001 reflections obtained in the XRD traces are ~10–11 Å without modification after saturation with ethylene glycol or heating at 550 °C. Therefore, the MIR and XRD results confirm the mica nature of these samples.

For synthesis in a reaction medium containing 28 mol.% of ethanol, the TEM images display a poorly crystallized sample with a Si/Mg weight ratio of ~0.78, similar to lizardite (weight ratio Si/Mg of ~0.78). This ratio and the XRD results suggest the synthesis of a poorly crystallized proto-serpentine (Andreani *et al.*, 2008). This 1:1 phyllosilicate is composed of only one tetrahedral sheet of silicon with one octahedral sheet of magnesium (T-O phyllosilicate) and is poorly crystalline.

Finally, the sample obtained in a reaction medium containing at least 50 mol.% ethanol is characterized by small polygonal particles composed mainly of magnesium oxide. These results confirm the synthesis of the brucite phase.

The synthesis of minerals adopting diverse structures according to the water/ethanol ratio of the solvent is demonstrated in Fig. 6. The layered mineral synthesized presents a brucitic structure (O), a brucitic structure associated with a Si-tetrahedral sheet (T-O) or a brucitic sheet inserted between two Si-tetrahedral sheets (T-O-T). Therefore, we demonstrated that the introduction of ethanol in the supercritical reaction medium modifies the metasilicate solubility in relation to the evolution of the dielectric constant of the water/ethanol mixture as a function of its composition, with a direct consequence on the formation of tetrahedral sheets of silicon (Akerlof, 1932; Akerlof & Short, 1936; Albright & Gosting, 1946; Rochester, 1972; Karaskova & Mollin, 1993; Fernández *et al.*, 1995; Bandura & Lvov, 2005).

This continuous method is quick (requiring only a few tens of seconds), sustainable and scalable and gives access to high-quality nanostructured minerals with unique physicochemical properties that cannot be obtained with other synthetic methods. Specifically, this process, using solvothermal treatment, enables us to control the structure of the layered material synthesized. This innovative route provides the first proof of synthesis in a few tens of seconds of various minerals in a continuous process simply by varying the solvent composition in the water/ethanol system. This appears to be a promising approach for preparing new synthetic minerals with tuneable layered structures.

ACKNOWLEDGMENTS

The authors acknowledge sincerely the reviewers for their constructive and helpful comments, E. Lebraud for XRD analyses and M. Lahaye for microprobe analyses. The authors also acknowledge financial support from Imerys Company for the PhD grant of M. Claverie. Lastly, we acknowledge the Conseil Régional Nouvelle-Aquitaine.

REFERENCES

Akerlof G. (1932) Dielectric constants of some organic solvent–water mixtures at various temperatures. *Journal of the American Chemical Society*, **54**, 4125–4139.

Akerlof G. & Short O.A. (1936) The dielectric constant of dioxane–water mixtures between 0 and 80°. *Journal of the American Chemical Society*, **58**, 1241–1243.

Albright P.S. & Gosting L.J. (1946) Dielectric constants of the methanol–water system from 5 to 55°. *Journal of the American Chemical Society*, **68**, 1061–1063.

Andreani M., Grauby O., Baronnet A. & Muñoz M. (2008) Occurrence, composition and growth of polyhedral serpentine. *European Journal of Mineralogy*, **20**, 159–171.

Aymonier C., Slostowski C., Dumas A., Micoud P., Le Roux C. & Martin F. (2015) Process for the Continuous Preparation of Phyllomineral Synthetic Particles – WO 2015159006 Al.

Aymonier C., Philippot G., Erriguible A. & Marre S. (2018) Playing with chemistry in supercritical solvents and the associated technologies for advanced materials by design. *The Journal of Supercritical Fluids*, **134**, 184–196.

Bandura A.V. & Lvov S.N. (2005) The ionization constant of water over wide ranges of temperature and density. *Journal of Physical and Chemical Reference Data*, **35**, 15–30.

Barr-David F. & Dodge B.F. (1959) Vapor–liquid equilibrium at high pressures. The systems ethanol–water and 2-propanol–water. *Journal of Chemical & Engineering Data*, **4**, 107–121.

Bazaev A.R., Abdulagatov I.M., Bazaev E.A. & Abdurashidova A. (2007) (p, v, T, x) Measurements of $\{(1-x)H_2O + xC_2H_5OH\}$ mixtures in the near-

https://doi.org/10.1180/clm.2018.36 Published online by Cambridge University Press

critical and supercritical regions. *The Journal of Chemical Thermodynamics*, **39**, 385–411.

Bergaya F. & Lagaly G. (2006) General introduction: clays, clay minerals, and clay science. Pp. 1–18 in: *Handbook of Clay Science* (F. Bergaya, B.K.G. Theng & G. Lagaly, editors). Elsevier, New York, NY, USA.

Carretero M.I. (2002) Clay minerals and their beneficial effects upon human health. A review. *Applied Clay Science*, **21**, 155–163.

Cecilia J.A., García-Sancho C., Vilarrasa-García E., Jiménez-Jiménez J. & Rodriguez-Castellón E. (2018) Synthesis, characterization, uses and applications of porous clays heterostructures: a review. *The Chemical Record*, **18**, 1085–1104.

Cirillo G., Kozlowski M.A. & Spizzirri U.G. (2018) *Composite Materials for Food Packaging*. John Wiley & Sons, Hoboken, NJ, USA.

Claverie M., Dumas A., Careme C., Poirier M., Le Roux C., Micoud P., Martin F. & Aymonier C. (2018) Synthetic talc and talc-like structures: preparation, features and applications. *Chemistry – A European Journal*, **24**, 519–542.

Diez-Garcia M., Gaitero J.J., Dolado J.S. & Aymonier C. (2017) Ultra-fast supercritical hydrothermal synthesis of tobermorite under thermodynamically metastable conditions. *Angewandte Chemie*, **56**, 3162–3167.

Ding Z., Kloprogge J.T., Frost R.L., Lu G.Q. & Zhu H.Y. (2001) Porous clays and pillared clays-based catalysts. Part 2: a review of the catalytic and molecular sieve applications. *Journal of Porous Materials*, **8**, 273–293.

Dumas A., Claverie M., Slostowski C., Aubert G., Careme C., Le Roux C., Micoud P., Martin F. & Aymonier C. (2016) Fast-geomimicking using chemistry in supercritical water. *Angewandte Chemie*, **55**, 9868–9871.

Fernández D.P., Mulev Y., Goodwin A.R.H. & Sengers J.M.H.L. (1995) A database for the static dielectric constant of water and steam. *Journal of Physical and Chemical Reference Data*, **24**, 33–70.

Grauby O., Baronnet A., Devouard B., Schoumacker K. & Demirdjian L. (1998) The chrysotile-polygonal serpentine lizardite suite synthesized from a $3MgO–2SiO_2$–excess H_2O gel. Presented at: *7th International Symposium on Experimental Mineralogy, Petrology and Geochemistry.*

Griswold J., Haney J.D. & Klein V.A. (1943) Ethanol–water system – vapor–liquid properties at high pressure. *Industrial & Engineering Chemistry*, **35**, 701–704.

Karaskova E. & Mollin U. (1993) Calculation of alkoxide and hydroxide ion activity ratios in the water–ethanol system 4. *Chemical Papers*, **37**, 156–159.

Konta J. (1995) Clay and man: clay raw materials in the service of man. *Applied Clay Science*, **10**, 275–335.

Laaksonen A., Kusalik P.G. & Svishchev I.M. (1997) Three-dimensional structure in water–methanol mixtures. *The Journal of Physical Chemistry A*, **101**, 5910–5918.

Marshall W.L. & Jones E.V. (1974) Liquid–vapor critical temperatures of several aqueous–organic and organic–organic solution systems. *Journal of Inorganic and Nuclear Chemistry*, **36**, 2319–2323.

Murray H.H. (2000) Traditional and new applications for kaolin, smectite, and palygorskite: a general overview. *Applied Clay Science*, **17**, 207–221.

Robert J.-L. & Kodama H. (1988) Generalization of the correlations between hydroxyl-stretching wavenumbers and composition of micas in the system $K_2O–MgO–Al_2O_3–SiO_2–H_2O$: a single model for trioctahedral and dioctahedral micas. *American Journal of Science*, **288-A**, 196–212.

Robert J.-L., Beny J.-M., Ventura G.D. & Hardy M. (1993) Fluorine in micas: crystal-chemical control of the OH-F distribution between trioctahedral and dioctahedral sites. *European Journal of Mineralogy*, **5**, 7–18.

Rochester C. (1972) The ionic products of water and methanol in methanol–water mixtures. *Journal of the Chemical Society, Dalton Transactions*, **1**, 5–8.

Schaef H.T., Loring J.S., Glezakou V.-A., Miller Q.R.S., Chen J., Owen A.T., Lee M.-S., Ilton E.S., Felmy A.R., McGrail B.P. & Thompson C.J. (2015) Competitive sorption of CO_2 and H_2O in 2:1 layer phyllosilicates. *Geochimica et Cosmochimica Acta*, **161**, 248–257.

Zazenski R., Ashton W.H., Briggs D., Chudkowski M., Kelse J.W., MacEachern L., McCarthy E.F., Nordhauser M.A., Roddy M.T. & Teetsel N.M. (1995) Talc: occurrence, characterization, and consumer applications. *Regulatory Toxicology and Pharmacology: RTP*, **21**, 218–229.

https://doi.org/10.1180/clm.2018.36 Published online by Cambridge University Press